Macromolecular Research

Article

DOI 10.1007/s13233-022-0059-z

www.springer.com/13233 pISSN 1598-5032 eISSN 2092-7673

Environmental Friendly Intumescent Flame Retardant Gives Epoxy Resin Excellent Fire Resistance and Mechanical Properties

Huan Wang[1]
Li Li[1]
Yan Kang[2]
Xue Yin[1]
Xuedi Lei[1]
Jing Yang[1]
Hui Xi[1]
Xueqing Xu[1]
Zhiwang Yang*[,1]
Ziqiang Lei*[,1]

[1] Key Laboratory of Polymer Materials of Gansu Province, Key Laboratory of Eco-Functional Polymer Materials, Ministry of Education, College of Chemistry and Chemical Engineering, Northwest Normal University, Lanzhou, 730070, P. R. China
[2] Department of Tibetan Medicine, University of Tibetan Medicine, Lhasa 850000, P. R. China

Received November 8, 2021 / Revised March 16, 2022 / Accepted March 21, 2022

Abstract: To reduce the fire hazard of epoxy resin (EP), PA-CS-M (where PA = phytic acid, CS = chitosan, M = Cu^{2+}, Co^{2+}, Al^{3+}, Zn^{2+}, Mn^{2+}) environmental friendly flame retardant is prepared by a simple and green method. By comparing the data after cone calorimetry test (CCT) of various composites, it is found that when 5 wt% PA-CS-Mn is added to EP, it has good flame retardant and smoke suppression performance. The peak heat release rate (pk-HRR) decreased by 38% and the smoke production rate (SPR) decreased by 33%. In addition, some toxic smoke such as CO has been significantly inhibited. The structures and morphologies of the materials were investigated by Fourier transform infrared (FTIR), X-ray diffraction (XRD), scanning electron microscopy (SEM), and X-ray photoelectron spectroscopy (XPS). When combined with expandable graphite (EG), it is found that when the ratio of PA-CS-Mn to EG is 1:5, the pk-HRR value and SPR value decreased by 69.8% and 66.6%, respectively. More importantly, the mechanical properties of the EP composites have also been greatly improved. The flexural modulus reaches 5.04 GPa, which is 52.3% higher than pure EP, and the flexural strength increases to 79.4 MPa, which also shows an increase of 41.4% as to the matrix.

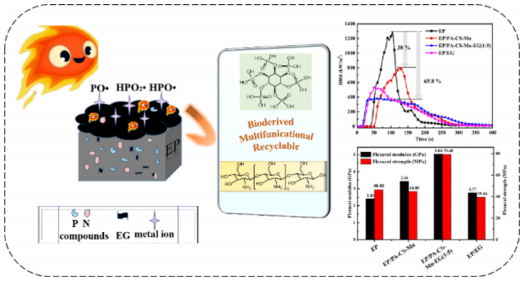

Keywords: intumescent flame retardant, phytic acid, chitosan, mechanical property, epoxy resins.

1. Introduction

As a widely used thermosetting resin material, epoxy resin has attracted more and more attention from researchers and industries. In the major industries close to human life, such as petrochemical industry, manufacturing industry, building materials, electronics and electrical appliances, epoxy resin with its excellent performance runs through all major fields.[1-3] But sometimes its flammability limits it to play a greater application value in some special fields, so it is generally necessary to add flame retardant in this kind of matrix to meet the needs of real life. In fact, the traditional halogen flame retardant can achieve better flame-retardant effect than halogen-free flame retardant. However, the harmful by-products produced during the combustion of materials often seriously endanger our living environment and human health. At this stage, clear laws and regulations have been issued to restrict the use of halogen-containing flame retardants, effectively improving the safe use of flame retardants. In recent times, the replacement of using toxic halogen-containing fire retardants (FRs) by eco-friendly and high efficiency phosphorus-containing flame retardants has attracted great attention.[4-8]

Phytic acid (PA), also known as an inositol hexaphosphate, has become one of the alternatives of halogen-free flame retardant in recent years due to its unique highly active phosphate groups in the structure with the phosphorus content of 28 wt%.[9-11] In addition, because of the strong chelating ability of phosphoric acid group in its molecule structure, it can complex with a variety of metal ions to improve the catalytic carbonization ability of the material.[12-14] Besides, it can also be well cross-linked with amino compounds in a compound to construct P-N flame retardant system.[15,16] So it can be employed to react with other organic groups with flame-retarding function, thus syn-

Acknowledgment: The research was financially supported by NSFC (52063026, 21563026), the Program for Changjiang Scholars and Innovative Research Team in University (IRT15R56), the Innovation Team Basic Scientific Research Project of Gansu Province (1606RJIA324), and the Science, Technology Program of Gansu Province (19JR2RA020) and Education Department of Gansu Province: Excellent Graduate Student "Innovation Star" Project (2021CXZX-001). We also thank the Key Laboratory of Eco-functional Polymer Materials (Northwest Normal University), Ministry of Education, and the Gansu International Scientific and Technological Cooperation Base of Water-Retention Chemical Functional Materials, for financial support.

***Corresponding Authors:** Zhiwang Yang (yangzw@nwnu.edu.cn), Ziqiang Lei (Leizq@nwnu.edu.cn)

thesizing various polymeric or hyperbranched efficient flame retardants to improve the flame retardant performance. Kundu *et al*. functionalized lignin and phytic acid biomass resources with graphene oxide (GO) and then used a one-pot deposition method to enhance the flame retardant properties of polyamide 66 (PA66) fabrics. The LOI value of the flame retardant PA66 reached 27%.[17] In addition, researchers have pointed out that phytic acid can replace ammonium polyphosphate (APP), one of the components of intumescent flame retardants, and exert excellent flame retardant effects in flame retardant systems. Li et al prepared melamine phytate (PAMA) nanosheets by hydrothermal method, and then further obtained PAMA-Mn nanosheets by chelating with metal ion Mn^{2+}. Further analysis of the flame retardant mechanism of PP composite shows that the expandable carbon layer produced by PP composite plays a great barrier role in the condensed phase. On the one hand, it can effectively isolate the heat exchange between the matrix material and the air, on the other hand, it can be used as an effective covering layer to prevent further combustion of the material.[9,18-19]

Chitosan is the second largest natural biodegradable polymer in the world after cellulose, consisting of β-(1-4) linked d-glucosamine and N-acetyl-d-glucosamine, mainly derived from exoskeletons of shell crustaceans and arthropods.[20-22] Such a readily sourced natural cationic polysaccharide has been demonstrated to act as a carbon source and blowing agent for intumescent flame retardants (IFR). And because of its rich amino and hydroxyl functional groups in its structure, it can react with many phosphorus-containing compounds, and it has a certain excellent carbonization effect and good thermal stability in many flame retardant systems. Compared with single-component chitosan, combining chitosan with other materials to form a synergistic flame retardant often achieves better flame retardant effect.[23,24] Many researchers have applied it to the flame retardant systems of polyvinyl alcohol,[25] polyethylene[26] and polylactic acid.[27] Mohamed Hassan *et al*. combined phosphoric acid, chitosan, and melamine to prepare intumescent flame retardants and found that peak heat release rate (pk-HRR) of polyethylene was effectively reduced through the cone calorimetry test (CCT), and then reduced the risk of fire.[26] Chen et al designed and synthesized a new type of environmentally friendly flame retardant through chitosan, cinnamaldehyde, 9,10-dihydro-9-oxa-10-phosphaphenanthrene-10-oxide (DOPO) and other raw materials and applied it to epoxy resin. The cone calorimetry test shows that the flame retardant has a great inhibitory effect on the smoke generation, which is 72% lower than that of pure epoxy resin. And the limiting oxygen index is increased by 7.6%, which is closely related to the excellent carbonization effect of chitosan.[28]

In recent years, metal ions have been used to improve the flame retardancy of materials because of their excellent catalytic carbonization.[29-32] Many researchers have found that phytic acid can also cross-link with most metal ions and positively charged matrices, such as Fe^{3+}, Zn^{2+}, Mn^{2+}, etc.[33] Liu[34] *et al*. used four different metal ions Fe^{2+}, Mn^{2+}, Al^{3+} and Cu^{2+} to modify humic acid (HA) and then applied it to flame retardant epoxy resin. When 10 wt% HA-Fe and HA-Mn were added, the LOI was changed from 21.2% increased to 26.6% and 25.3%, and pk-HRR decreased by 36% and 35.5%, respectively. Further research on the morphology of the carbon residue can show that a denser and more continuous carbonized layer is formed on the surface of the substrate, which indicates that the carbonization ability of HA is closely related to the catalytic effect of Fe and Mn. It not only provides environmental friendly components, but also forms a more stable structure through the interaction of positive and negative charges between chemical bonds. Therefore, adding metal elements to the polymer matrix can significantly increase the content of the carbon layer, and a high-quality carbon layer has a good barrier effect on inhibiting oxygen supply, inhibiting heat exchange, and hindering the release of flue gas.[35]

Based on this, an environmental friendly intumescent flame retardant was synthesized by combining phytic acid, chitosan and metal ions to protect epoxy resin matrix. Among them, the abundant hydroxyl groups in phytic acid and the amino groups in chitosan can chelate with metal ions to form a cross-linked network, which can play a role of flame retardant in gas and condensed phase in epoxy resin matrix. In the process of combustion, the carbon forming ability of polymer can be promoted and the thermal stability of polymer can be greatly improved. In addition, expandable graphite (EG), as a traditional halogen-free and efficient flame retardant, has been widely studied. However, the mechanical properties of the material are often seriously affected by the excessive addition of flame retardants. Therefore, it is particularly important to find a green and efficient flame retardant with good compatibility with the matrix material. Based on this, this study combined PA-CS-M (M=Cu^{2+}, Co^{2+}, Al^{3+}, Zn^{2+}, Mn^{2+}) and traditional halogen-free flame retardant EG to act on flame retardant epoxy resin. By choosing the appropriate proportion of PA-CS-Mn and EG, the flame retardant properties of epoxy resin (EP) have been well improved.

2. Experimental

2.1. Materials

Epoxy resins (EP) was supplied by Nantong Xingchen Synthetic Material Co. Phytic acid (PA, 70 wt%) was purchased from Shanghai Aladdin Biochemical Technology Co. Expandable graphite (EG) was received from Qingdao Tianhe Graphite Co. Anhydrous ethanol was supplied by Sinopharm Co. Zinc chloride was provided by Tianjin Kaitong Chemical Reagent Co. Aluminum trichloride hexahydrate was provided by Tianjin Guangfu Institute of Fine Chemicals. Copper chloride dihydrate and cobalt chloride hexahydrate were supplied by Shanghai Zhongqin Chemical Reagent co. Manganese chloride tetrahydrate was supplied by Tianjin Tianhe Chemical Reagent Factory. Diethylenetriamine (DETA) was supplied by Tianjin Kaixin Co. The deionized (DI) water used was prepared in our laboratory.

2.2. Methods

2.2.1. Preparation of PA-CS-M (M = Cu^{2+}, Co^{2+}, Al^{3+}, Zn^{2+}, Mn^{2+})

Take PA-CS-M (M = Mn^{2+}) as an example, where phytic acid, chitosan, and manganese chloride are used as raw materials to prepare an environmental friendly composite flame retardants.

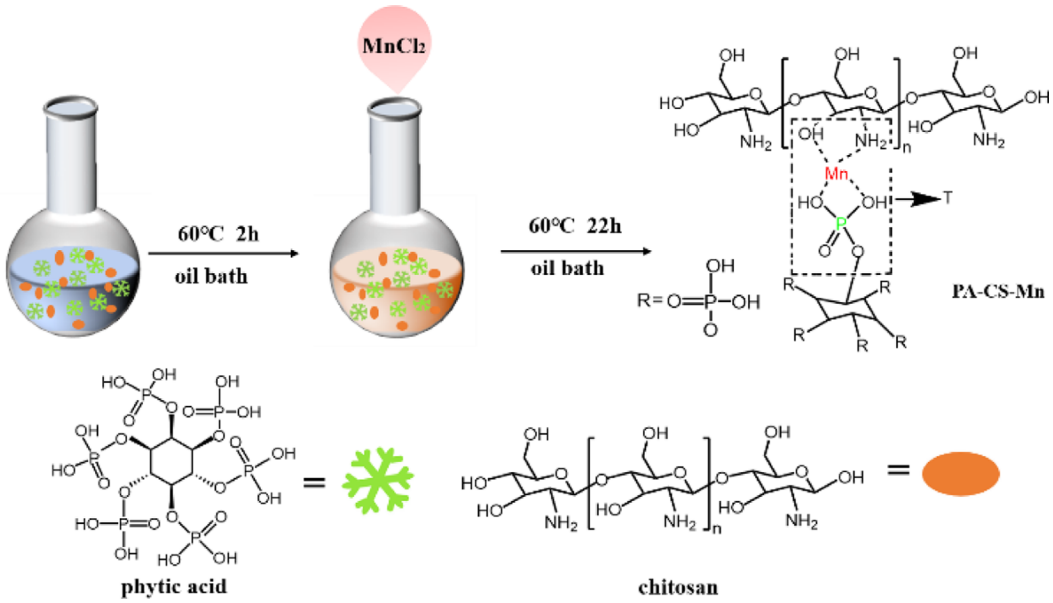

Scheme 1. Schematic illustration of the fabrication of PA-CS-Mn.

The synthesis of PA-CS-Mn flame retardant was illustrated in Scheme 1.

Firstly, 5 mL of phytic acid was dispersed in 50 mL of distilled water into a round-bottom flask with vigorous stirring at room temperature, and then 2 g of chitosan was added. The mixture was placed in a 250 mL round-bottom flask and heated in an oil bath at 60 ℃ for 2 h. After that, a certain amount of $MnCl_2$ was added and reacted for an additional 22 h, then cooled it to room temperature overnight to form a pale-yellow gel.

When 100 mL ethanol was added, a large amount of white powder appeared immediately in the round bottom flask. After filtration, the product was washed with ethanol and then freeze-dried. The preparation process of PA-CS-M (M = Zn^{2+}, Al^{3+}, Co^{2+}, Cu^{2+}) was the same as above. The reaction products of different metal salts with phytic acid and chitosan are relatively light, and the final yield difference is small. PA-CS-Mn is dark white powder, the yield is about 71%. PA-CS-Zn is white powder, the yield is 65%. PA-CS-Al is white powder, the yield is 69%, and PA-CS-Co is purple powder, the yield is 67%. PA-CS-Cu presents light blue powder with the lowest yield of 56%.

2.2.2. Preparation of EP composites

2.2.2.1. Preparation of EP/PA-CS-M

The epoxy-based nanocomposites containing the PA-CS-M flame retardant were prepared as follows. PA-CS-M flame retardant was dissolved in 15 mL of ethanol in a water bath at 70 ℃ firstly. After fully dispersed, 30 mL of epoxy resin was added and continued to stir evenly for another 30 min, then 3.4 mL of diethylenetriamine as curing agent was added to the mixture and the extra ethanol was removed by vacuum filter. The resulted glutinous mixture was then poured into a silicone oil- preheated mold to make a preformed sample with specific shape. The preformed sample was further treated through a programing heating stage. That is, it was firstly heated in an oven at 80 ℃ for 30 min, then the oven temperature was rose to 110 ℃ and the preformed sample was continuously cured for 3 h to get a final sample. In addition, the preparation process of EP/EG composites is consistent with the preparation process of EP/PA-CS-Mn flame retardants. Among them, EP/PA-CS-Mn is simply represented as EP1, and EP/EG is represented as EP8.

2.2.2.2. Preparation of EP/PA-CS-Mn-EG

Select PA-CS-Mn and EG with different mass ratios (1:1, 1:3, 1:5, 1:7, 3:1, 5:1) to replace the single-component 5 wt% PA-CS-Mn as an added component. After that, it was added to the EP system respectively, and the subsequent debubbling and heating process was consistent with the preparation process of the above-mentioned preparation of EP/PA-CS-Mn composites. When PA-CS-Mn and EG were co-added into EP, EP/PA-CS-Mn-EG composites were obtained. Among them, EP/PA-CS-Mn-EG with different mass ratios (1:1, 1:3, 1:5, 1:7, 3:1, and 5:1) are expressed as EP2, EP3, EP4, EP5, EP6 and EP7 in turn.

2.3. Instruments

2.3.1. Characterization of the samples

Fourier transform infrared (FTIR) spectroscopies were recorded in the scanning range of 400 to 4000 cm^{-1} (KBr disks) at room temperature on a Nicolet NEXUS 670 spectrometer. X-ray diffraction (XRD) was carried out on a Rigaku D/max-2400 X-ray powder diffractometer (using Ni-filtered Cu Kα radiation at 40 kV and 40 mA). The surface morphology of the samples was investigated by field emission scanning electron microscopy (FE-SEM, Ultra Plus, Carl Zeiss, Germany, after gold sputtering on a JSM 5600 LV instrument) and transmission electron microscopy (TEM) (FEI TECNAI G2 TF20, America). X-ray photoelectron spectroscopy (XPS) was carried out by an X-ray photoelectron spectrometer (PHI-5702, America). The thermogravimetric analysis (TGA) curves were analyzed with a Netzach STA449C thermogravimetric in N_2 atmosphere with a heating rate of 10 ℃/min from room temperature to 800 ℃.

2.3.2. Properties of the samples

Limiting oxygen index (LOI) data of all samples were performed on a Model HC-2C oxygen index meter (Jiangning Analysis Instrument Company, China) on a sheet with the dimension of 130 × 6.5 × 3.2 mm according to the standard oxygen index test of ASTM D2863-97. The UL-94 vertical burning test was conducted using a Model FT 0082 horizontal and vertical burning tester (UK) with the dimension of 127 × 12.7 × 3 mm according to the UL-94 test standard of ASTM D3801-1996. The cone calorimeter test data were evaluated by a cone calorimeter of FTT 0402 (UK) device at a heat flux of 50 kW/m^2 according to ISO 5660-1 standard with the dimension of 100 × 100 × 3 mm. The experimental error for all the mentioned parameters is ± 5%. The mechanical properties were tested by WDW-2C electronic universal testing machine at room temperature according to GB/T1040-92 standard with the dimension of 80 × 10 × 4 mm.

3. Results and discussion

3.1. Studies on PA-CS-M (M = Cu^{2+}, Co^{2+}, Al^{3+}, Zn^{2+}, Mn^{2+})

The FTIR spectra of PA-CS-M synthesized with different metal ions are shown in Figure 1. It is obvious that all the PA-CS-M FTIR spectra have a broadband peak at 3400 cm^{-1}. For phytic acid, it is mainly caused by the stretching vibration peak of O-H in the molecule. For chitosan, it is the characteristic peak of -OH and -NH_2 functional groups, which also indicates that there are abundant -OH and -NH_2 in PA-CS-M. The above analysis shows that there is a certain interaction among phytic acid, chitosan and metal ions, which can form a good cross-linking network, and can be proved in the following spectrum analysis. In addition, compared with the stretching vibration peaks of P-O at 1043 cm^{-1} and P-O-C at 966 cm^{-1}, and the bending vibration peaks of P-O at 503 cm^{-1} in phytic acid, it can be found that the stretching vibration peak of P-O (P-O-Mn) moves to 1078 cm^{-1} and the bending vibration peak of P-O-C moves to 995 cm^{-1} in PA-CS-Mn. The bending vibration peak of P-O moves to 522 cm^{-1}, and the infrared spectra of other metal ions are similar to that of PA-CS-Mn. All of them have wave number transfer in different ranges, indicating that phytic acid participates in the chelation process with metal ions. In another component of chitosan, the absorption

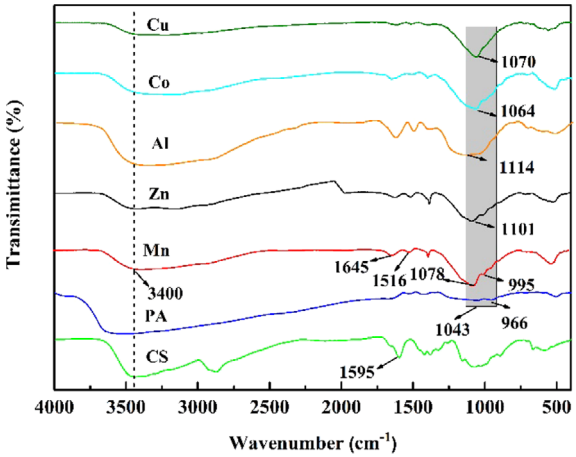

Figure 1. FTIR spectra of PA, CS, PA-CS-M (M = Cu^{2+}, Co^{2+}, Al^{3+}, Zn^{2+}, Mn^{2+}).

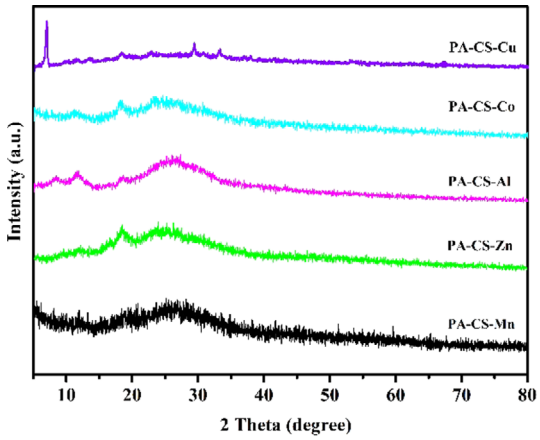

Figure 2. XRD patterns of PA-CS-M (M = Cu^{2+}, Co^{2+}, Al^{3+}, Zn^{2+}, Mn^{2+}).

peak of -NH_2 is 1595 cm^{-1}, while the absorption peak of PA-CS-Mn is 1516 cm^{-1}. This wave number shift also indicates that Mn^{2+} is complexed with -NH_2 in chitosan. Thus, we can prove that the complex of phytic acid, chitosan and metal ions has been successfully combined to synthesize PA-CS-M ternary composite flame retardant.

X-ray diffraction (XRD) is a method to obtain the composition and internal atomic or molecular structure of materials by diffraction patterns. We can judge the properties of synthetic materials mainly by the change of diffraction peak intensity and the influence of other components on the crystal shape.[36-40] The XRD patterns of PA-CS-M (M = Cu^{2+}, Co^{2+}, Al^{3+}, Zn^{2+}, Mn^{2+}) are shown in Figure 2. Except for PA-CS-Cu complex, which has a sharp and obvious characteristic peak at about 2θ = 5°, other metal ion complexes all show a wide diffraction peak in the range of 2θ = 20-35°, which indicates that the synthesized materials are amorphous-structured.

In order to further study the element types and electronic valence states of the synthesized flame retardants, we performed the XPS analysis of PA-CS-Mn complexes. The test results are as follows. From the survey spectrum of Figure 3(a), it can be found that PA-CS-Mn contains five elements including C, O, N, P, and Mn. By fitting the spectrum of Mn_{2p}, N_{1s} and P_{2p} with Gauss method, respectively, we can get a better understanding of the coordination mode between the atoms. In the spectrum of Mn_{2p} (Figure 3(b)), two peaks appear at 642.08 and 654.08 eV correspond to the characteristic peaks of Mn_{2p} 3/2 and Mn_{2p} 1/2, respectively.[9] There are also two broadband peaks around them, which belong to their respective satellite peaks, indicating that Mn^{2+} is successfully coordinated with the legands in the complex. In the N_{1s} spectrum (Figure 3(c)), the peak with binding energy of 400.03 eV is the characteristic peak of -NH_2 group in chitosan. After complexing with Mn^{2+}, a new peak appeared at 397.95 eV.[41]

In the P_{2p} spectrum (Figure 3(d)), it is obvious that two characteristic peaks are at 133.08 and 133.95 eV, which are mainly caused by the existence of P-O bond and phosphate group in phytic acid.[42] In addition, two peaks of 530.79 eV and 531.82 eV can also be fitted from O_{1s} (Figure 3(e)), corresponding to O-Mn and O-H bonds respectively. Through the above XPS photoelectron spectroscopy analysis of the valence bond of each element, it can be clearly seen that the three components of phytic acid,

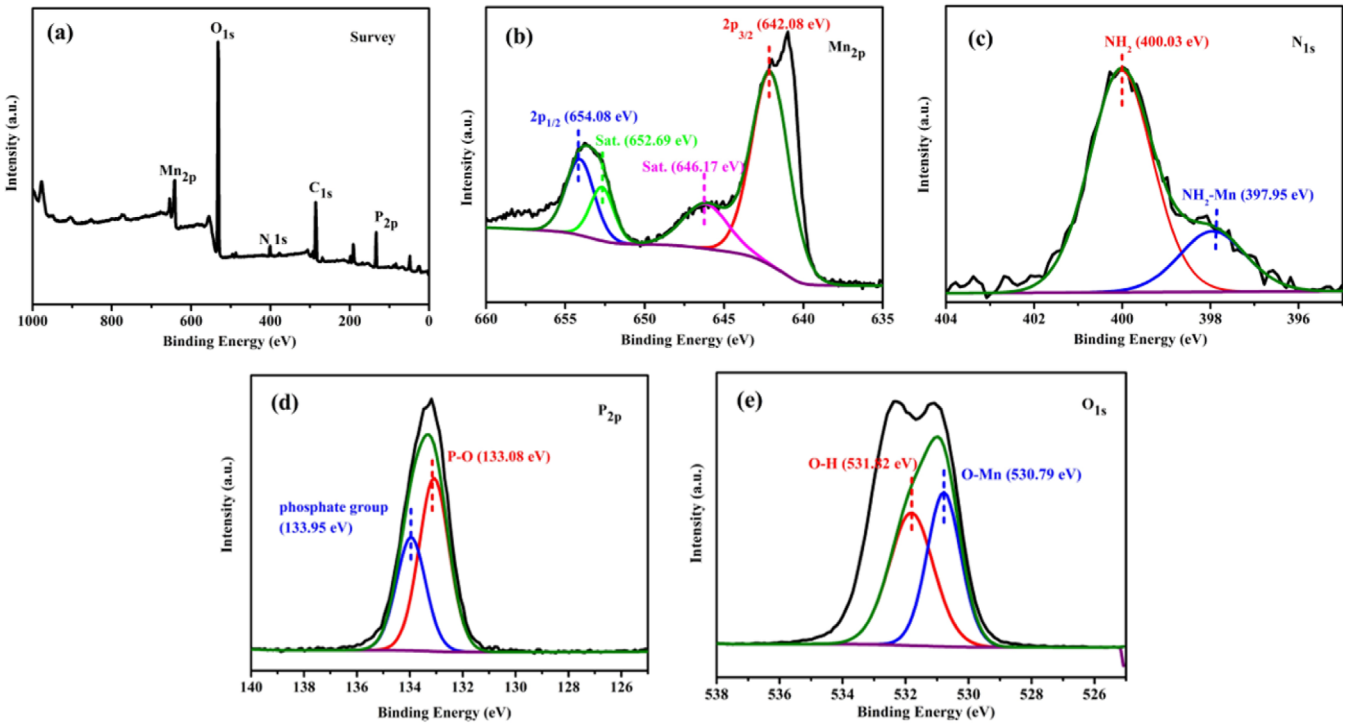

Figure 3. XPS spectra for the PA-CS-Mn, survey (a), Mn_{2p} (b), N_{1s} (c), P_{2p} (d), and O_{1s} (e).

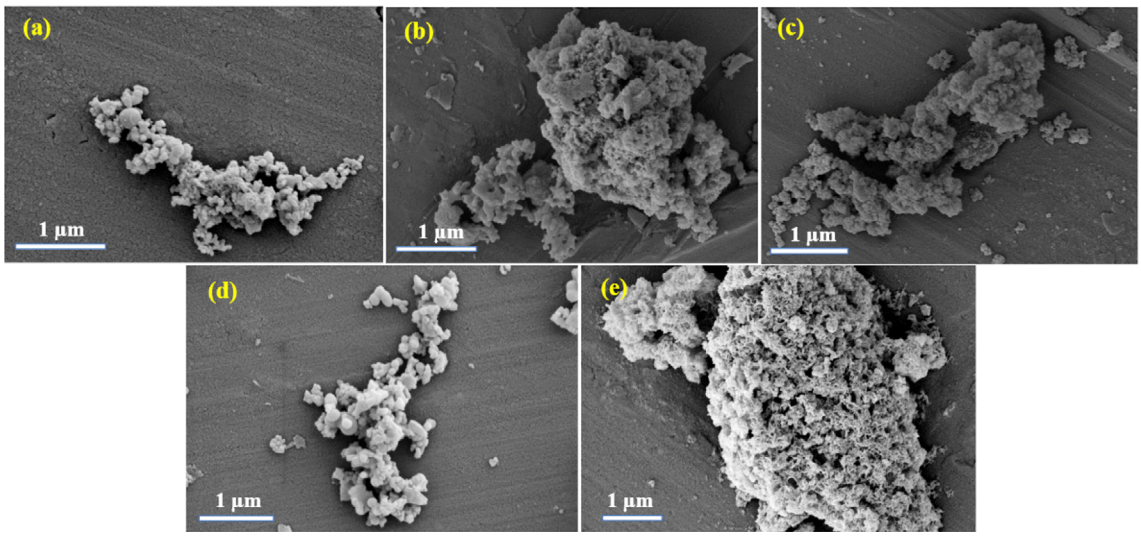

Figure 4. SEM images of PA-CS-M (M = Mn^{2+}(a), Zn^{2+}(b), Al^{3+}(c), Co^{2+}(d), Cu^{2+}(e)).

chitosan and metal ion Mn^{2+} have been successfully combined to prepare PA-CS-Mn complex.

The scanning electron microscopes (SEM) of PA-CS-M (M = Cu^{2+}, Co^{2+}, Al^{3+}, Zn^{2+}, Mn^{2+}) are shown in Figure 4. By comparing the SEM images of different metal complexed, it can be found that all of the complexes show as soft aggregation powders with and porous structures, which will bring prospectively good compatibility of the flame retardant and the polymer matrix (Figure 4(a)). Of all these complexes, the nanostructure of PA-CS-Mn is differed from others with its looser and smoother morphology. This looser and smoother morphology may bring more close contact of the complex and the matrix, and therefore it can be prophesied PA-CS-Mn may show better flame retardancy in the applications.

3.2. Thermal properties of EP and EP composites

The thermal decomposition behaviors of EP and its composites were investigated by the TGA. Figure 5 gives the TGA thermograms of the EP, EP/PA-CS-Mn, EP/PA-CS-Mn-EG (1:5), and EP/EG composites under nitrogen atmosphere. Pure EP mainly exhibits two-stage thermal weight loss between 30-120 ℃ and 300-500 ℃, and its corresponding mass loss is 2.2% and 26.2%, respectively, which means that its thermal stability is the worst. However, with the addition of flame retardants, the carbon-forming ability of the EP surface can be improved, so the thermal stability of the material is improved. Compared with pure EP, the mass loss of PA-CS-Mn reaches 6.2%, which may be due to the fact that the flame retardant effect of phosphorus contain-

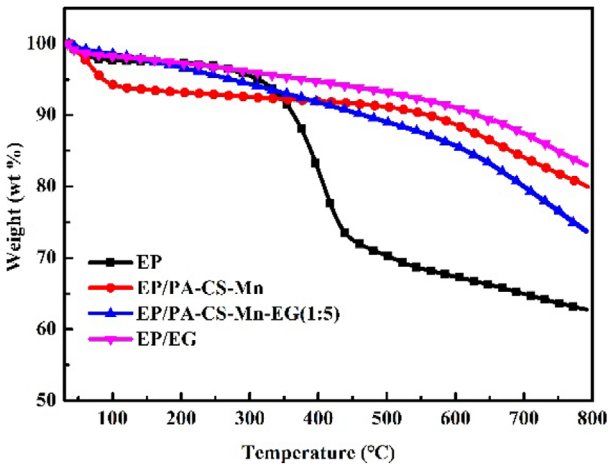

Figure 5. TGA profiles of EP, EP/PA-CS-Mn, EP/PA-CS-Mn-EG (1:5), EP/EG hybrids under nitrogen atmosphere.

ing radicals has not been exerted at the beginning of combustion. But the initial decomposition temperature of PA-CS-Mn is delayed, and the maximum decomposition rate during the whole combustion process is decreased, and the carbon residue increases obviously after 800 ℃. Furthermore, the carbon layer on the surface of the EP/PA-CS-Mn composite does not significantly decrease compared to EG with conventional high-quality carbon layer. This indicates that both phytate-based phosphorus compounds and CS can promote the formation of high-quality carbon layers. The rapid char formation inhibits the degradation rate of the flame retardant and epoxy matrix, thereby preventing the spread of heat and mass.[43,44] If only EG is added to EP, at the stage of 100-300 ℃, EG will immediately have an expansive effect, which improves the carbonization ability and exerts a flame retardant effect. It can also be confirmed by the electron microscopy and Raman spectra of carbon residue. When the ratio of PA-CS-Mn and EG is 1:5, the thermal decomposition process of PA-CS-Mn is almost similar to that of EG. This indicates that both of them have synergistic effect, which can jointly play the intumescent flame retardant mechanism of PA and EG, and protect the thermosetting materials of EP matrix with their excellent carbonization ability.

3.3. Cone calorimetry test (CCT)

Generally speaking, cone calorimetry is an effective method to evaluate the combustion behavior of flame retardant materials. It mainly aims at testing and evaluating several key factors, including the peak heat release rate (pk-HRR), total heat release (THR), smoke producing rate (SPR), total smoke producing (TSP), etc.[45-47] The test data of EP composite [EP/PA-CS-M (M = Cu^{2+}, Co^{2+}, Al^{3+}, Zn^{2+}, Mn^{2+})] are listed in the Figure 6 and Table 1.

From the pk-HRR curves in Figure 6(a) can be seen that the pk-HRR values of the samples with the adding of flame retardants are obviously lower than those of pure EP. The flame retardancy of different metal ions complexed with phytic acid and chitosan is not the same. It can be clearly seen that the peak heat release rate (pk-HRR) of unmodified epoxy resin reaches 1294 kW/m^2. After the incorporation of PA-CS-Mn, compared with other metal ions, its pk-HRR value drops to 799 kW/m^2 with about 38% decreasing. From the total heat release (THR) curve in Figure 6(b), it can be seen that the introduction of most different metal salt-based compound composites results in varying degrees of THR decrease. Among them, the decrease of THR value of EP/PA-CS-Mn is not obvious, but it may be related to delaying the ignition time of EP composites. Of course, in addition to the amount of heat released, the amount of smoke producing rate (SPR) is also another key factor in investigating the flame retardancy. It can be seen from Figure 6(c) that the SPR value of pure EP is 0.33 m^2/s, and the SPR value of EP composites is found to decrease after adding flame retardant. Among them, the SPR value of EP/PA-CS-Mn is reduced to 0.22 m^2/s, which is about 33% lower than that of pure EP, indicating that the EP/PA-CS-Mn complex has the best flame retardant performance. In addition, from the CO production (COP) rate in Figure 6(d), it can also be seen that the PA-CS-Mn flame retardant has a great inhibitory effect for the producing of CO, this will greatly reduce the emission of toxic smoke during a combustion process, and therefore, earning people the precious time to escape from the fire.

The CCT data of EP and its composite materials are shown in the following Table 1, including ignition time (TTI), peak heat release rate (pk-HRR), time to peak heat release rate (Time to pk-HRR), total heat release (THR), smoke production rate (SPR), CO production rate (COP), fire growth rate (FGR) index and the amount of residual carbon remaining after combustion. Generally speaking, the longer the ignition time and the time to reach the peak heat release rate, the lower the risk of fire. The pristine EP shows a TTI value of 41 s. Compared with other metal complexes, the addition of PA-CS-Mn can slightly delay the time of fire. The pk-HRR of the composites after the adding of the flame retardant with different metal complexes can prove that the metal complexes do have excellent catalytic carbonization ability during the combustion process, so that the material can exert a better flame retardancy. Also, as can be seen from the

Table 1. Combustion parameters obtained from CCT

Sample	TTI (s)	pk-HRR (kW/m^2)	Time to pk-HRR (s)	THR (MJ/m^2)	SPR (m^2/s)	COP (g/s)	FGR (kW/m^2s)	Char yield (wt%)
EP	41	1294	105	84.72	0.33	0.041	12.32	5.40
EP/PA-CS-Mn	51	799	125	81.90	0.22	0.020	6.39	7.20
EP/PA-CS-Zn	18	996	90	75.26	0.31	0.027	11.06	3.50
EP/PA-CS-Al	16	958	80	78.34	0.29	0.026	11.95	2.10
EP/PA-CS-Co	22	1123	110	93.51	0.30	0.033	10.20	3.10
EP/PA-CS-Cu	18	1139	75	75.24	0.31	0.033	15.18	5.50

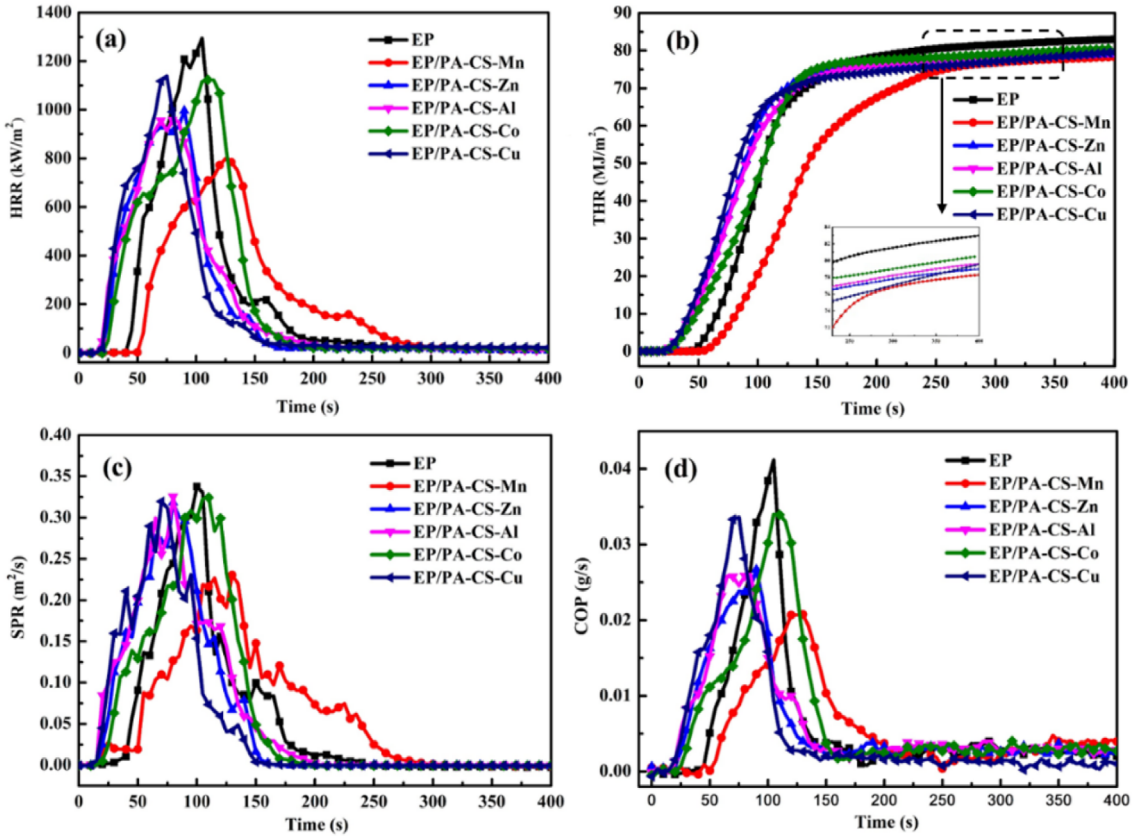

Figure 6. HRR (a), THR (b), SPR (c), and COP (d) of EP composites.

Table 2. Combustion parameters obtained from CCT[a]

Sample	EP (g)	PA-CS-Mn (g)	EG (g)	pk-HRR (kW/m^2)	SPR (m^2/s)	Char yield (wt%)
EP	100	0	0	1294	0.33	5.4
EP1	80	20.0	0	799	0.22	7.2
EP2 (1:1)	80	10.0	10.0	863	0.26	14.5
EP3 (1:3)	80	5.0	15.0	691	0.20	9.2
EP4 (1:5)	80	3.3	16.7	390	0.10	14.4
EP5 (1:7)	80	2.5	17.5	453	0.11	10.6
EP6 (3:1)	80	15.0	5.0	871	0.27	6.8
EP7 (5:1)	80	16.7	3.3	865	0.25	9.0
EP8	80	0	20.0	532	0.13	11.1

[a]In each sample, 3.4 g of diethylenetriamine (DETA) was added as curing agent.

table, the THR values of the EP/PA-CS-M composites are different. Generally speaking, the lower the THR value, the better the flame retardant effect. But it is also unavoidable that as the time for the material to reach its peak heat release rate increases, the heat release may increase. Therefore, it can be seen from Table 1 that the THR value of EP/PA-CS-Mn is still very high. The FGR index, calculated by the ratio between pk-HRR and the Time to pk-HRR, is usually used to assess the flame propagation rate of a material. The lower the FGR value, the lower the fire risk. The data in the comparison table clearly shows that PA-CS-Mn flame retardant has the best heat resistance during the combustion process. At the same time, combined with the amount of residual carbon, it can be found that the mass loss of the carbon layer of the EP/PA-CS-Mn composite is the least. The thicker the carbon residue left in this way, the lower the risk of fire.[48,49] During the combustion process of the EP/PA-CS-Mn composite material, a relatively high-quality and dense carbon layer will be continuously generated on the surface of the material, which inhibits the heat exchange between the inside and outside of the material. Once the material is effectively inhibited from further burning, the best flame retardant effect is often achieved.[50,51]

In order to further improve the flame retardancy of the EP matrix, we continue to optimize the composition of the EP/PA-CS-Mn composite. Therefore, EG, which is more common and has good flame retardancy, is selected as an additive component and added to the EP composites, and the flame retardancy of the material is further improved. As can be seen from Table 2 and Figure 7(a), the pk-HRR value of the EP8 composite dropped

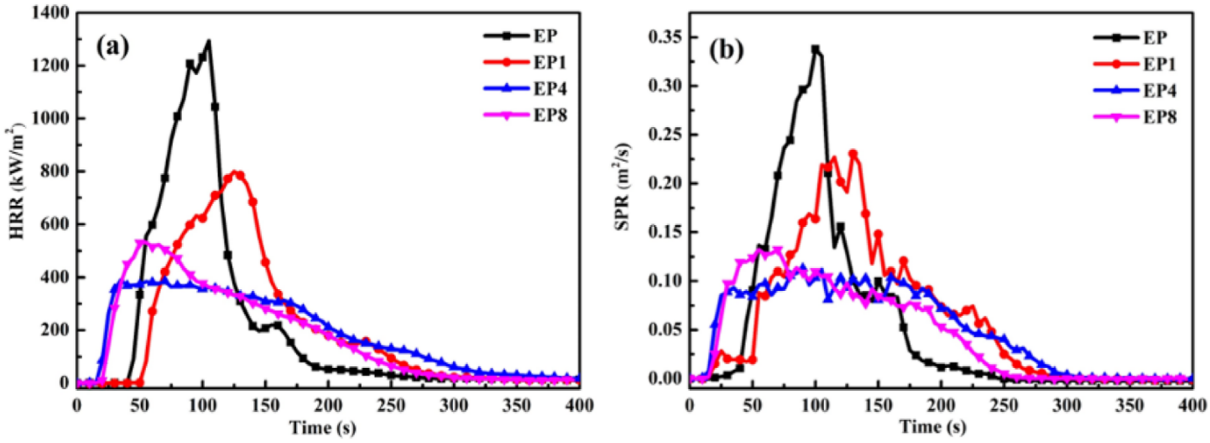

Figure 7. HRR (a) and SPR (b) of EP composites.

significantly from 1294 kW/m^2 to 532 kW/m^2 after only EG was added to the EP (Entry 9). This is mainly because of the forming of a relatively high dense carbon layer, which will isolate the heat in a combustion through a condensed phase fire-retardant mechanism. By change the ratio of PA-CS-Mn to EG, it shows that with the optimizing ratio of 1:5 (PA-CS-Mn-EG), the pk-HRR value of EP/PA-CS-Mn composites is reduced by 69.8%, and the SPR value is also reduced by 66.6% (Entry 5).This shows that in this flame-retardant system, phytic acid, chitosan, metal complex and EG together exert the flame-retardancy, which can indeed achieve relatively excellent fire-retardant performance.

The LOI values and UL-94 grades of different samples were measured to assess the flame retardancy. In Figure 8, the unmodified EP shows a LOI value of 19.0%. When only of PA-CS-Mn flame retardant is added, the LOI value does not change significantly. But when specific proportions of 1:5 of PA-CS-Mn to EG (w/w) were added, the oxygen index value increased to 22%. However, single addition of EG gives a lightly lower LOI value of 21.5%, it shows that the best flame retardant performance can be obtained only when PA-CS-Mn and EG work together. The vertical combustion test, like the limiting oxygen index method, can also be used to evaluate the flame retardant properties of materials. UL-94 judges the ability of a material to extinguish the flame after being ignited based on phenomena such as burning speed and time, and anti-dripping ability.[52,53] Table 3 shows the vertical combustion test results of EP and its composites. Pure EP burns for a long time and cannot self-extinguish. At the same time, it is accompanied by serious smoke and molten water dripping. It fails to pass the grade test. However, after adding the EP composite material, the burning time of the material is reduced, and there is no more dripping phenomenon, all of which have passed the V-1 level test. By comparison, it is found that the damage of the EP/PA-CS-Mn-EG

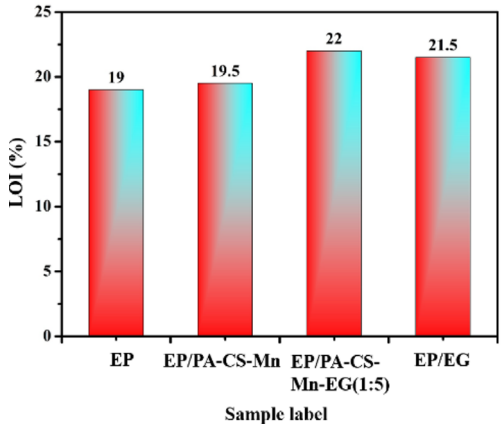

Figure 8. LOI values of pure EP and EP composites.

(1:5) sample is the smallest. It can be seen that when PA-CS-Mn and EG act together in EP, it will have a positive impact on the flame retardancy of EP.

3.4. Char residue analysis of different composites

As we all know, the microscopic morphology of carbon residue can well reflect the heat release behavior of the polymer matrix during the combustion process. Therefore, we conducted a CCT analysis on different sample such as EP, EP/PA-CS-Mn, EP/PA-CS-Mn-EG (1:5), and the SEM images as well as Raman spectroscopy analysis on the remaining carbon residue, the results were shown in Figure 9. Obviously, EP is almost completely burned, and the internal carbon residue is loose and porous (Figure 9(a), 9c). After adding PA-CS-Mn flame retardant, it is found that the remaining carbon layer after combustion is continuous and dense (Figure 9(b), 9(e)). Compared with pure EP combustion

Table 3. UL-94 results of pure EP and flame-retardant EP composites[a]

Sample	EP (g)	Flame retardant (g)	EG (g)	UL-94 rating
EP	100	0	0	NR
EP/PA-CS-Mn (EP1)	98	2	0	V-1
EP/PA-CS-Mn-EG (1:5) (EP4)	88	2	10	V-1
EP/EG (EP8)	98	0	2	V-1

[a]In each sample, 3.4 g of diethylenetriamine (DETA) was added as curing agent.

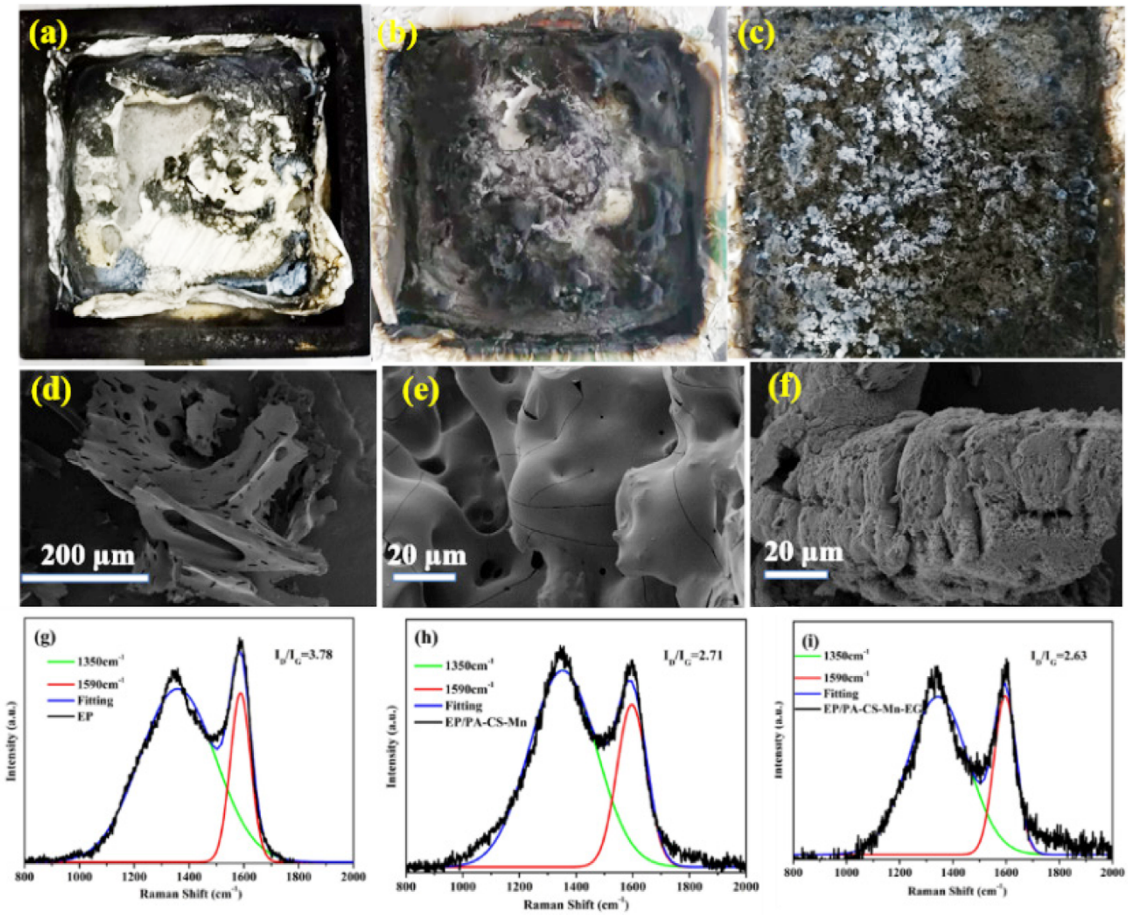

Figure 9. The digital photos, SEM images and the corresponding Raman spectra of EP (a, d, g), EP/PA-CS-Mn (b, e, h), EP/PA-CS-Mn-EG (1:5) (c, f, i) of the burning residues after CCT analysis.

products, there are only a few small holes on the surface of the residual carbon. Therefore, a dense protective layer is formed to isolate the heat transfer between the substrate and the air and, consequently, prevents the material from further burning. This is mainly because the abundant phosphoric acid groups and metal ions in the combustion work together to improve its catalytic carbonization ability, so it can achieve better Flame retardant effect. From Figure 9(c) and Figure 9(f) it can be found that after adding PA-CS-Mn and EG, the content of the remaining carbon layer after burning is relatively high, which is mainly due to the expansive of EG in the combustion.[42] Therefore, we can see that the combustion products have a worm-like structure, and the residue is firm and compact enough to obtain better protection of the matrix material.

The Raman spectra of the burning residues after CCT analysis of EP, EP/PA-CS-Mn, EP/PA-CS-Mn-EG (1:5) shows that all the samples have two obvious characteristic peaks at 1350 cm^{-1} and 1590 cm^{-1}, respectively, which are corresponding to the D band and the G band of the burning residues. The degree of graphitization of residual coke is determined by the ratio of the peak areas of D and G, i.e. I_D/I_G. Herein, the lower the I_D/I_G ratio is, the higher the graphitization degree of the residual char will be. In this way, the stronger the carbonization ability, the better the flame retardant performance of the material. The I_D/I_G values of EP, EP/PA-CS-Mn, EP/PA-CS-Mn-EG (1:5) are 3.78, 2.71, 2.63, respectively. Obviously, the addition of EP/PA-CS-Mn and EP/PA-CS-Mn-EG (1:5) composites can greatly improve the degree of graphitization of the residues. Since the carbon layer with a high degree of graphitization is more stable and not easy to be oxidized, it can block heat transfer and improve the flame retardant performance of the material.

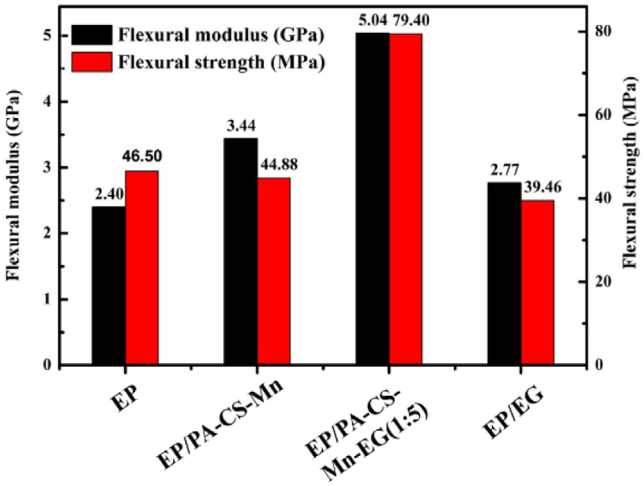

Figure 10. Mechanical properties of pure EP and EP composites.

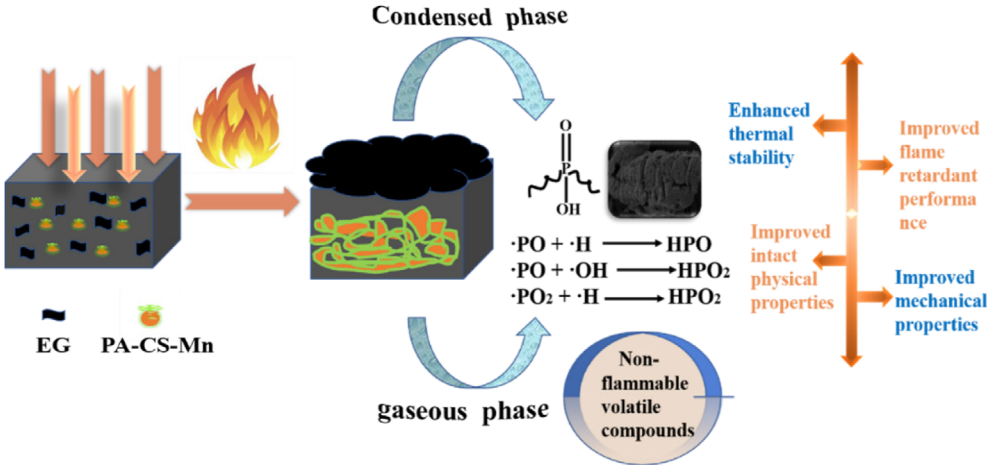

Scheme 2. Illustration of the fire retardance mechanism of EP/PA-CS-Mn-EG composite.

3.5. Compatibility and mechanical properties

The mechanical property of a material often play an important role in its daily application. The following Figure 10 shows the mechanical performance of EP and its composite materials. It found that PA-CS-Mn is helpful to enhance the flexural modulus of EP, and has little effect on its flexural strength. It can be seen that the addition of PA-CS-Mn flame retardant in EP can still maintain good compatibility with the matrix material. This may be the presence of amine groups in chitosan and phosphate groups in phytic acid. Both can react with the epoxy groups of EP, thus maintaining the good mechanical properties of EP composites. In addition, the addition of EG alone cannot greatly change the mechanical properties of the material. It has been reported in the literature that this is mainly related to the rough surface of EG after fracturing.[47] However, when PA-CS-Mn and EG work together, the mechanical properties of the material are greatly improved, the flexural modulus reaches 5.04 GPa, which is 52.3% higher than that of pure EP, and the flexural strength also increases to 79.4 MPa, which is 41.4% higher than that of pure EP. This can also be seen from the SEM image of the residual carbon, the fracture surface presents a solid and compact carbon layer. Therefore, the addition of the flame retardant PA-CS-Mn not only improves the defects of the traditional flame retardant of EG, strengthens the interaction force with EP and provides better compatibility, but also improves the mechanical properties of EP. That is, there exists obvious synergistic effect between PA-CS-Mn and EG for the improvement of the flame retardancy of EP.

3.6. Flame-retardancy mechanism

Through the above analysis, it can be found that the addition of PA-CS-Mn flame retardant and EG can indeed improve the flame retardancy of the material. Scheme 2 is a schematic diagram of the flame-retardant mechanism of EP and its composites. In the condensed phase, the phosphoric acid groups in phytic acid, the added EG and the PA-CS-Mn complex can act as a protective barrier together to produce an expanded carbon layer on the surface of the material matrix. During this reaction process, the P-containing compounds produced during the combustion process can accelerate the formation of the carbon char layer. At the same time, the ordered worm-like-structured graphite flakes produced on the surface can be used as a barrier to prevent heat and oxygen transfer, which can effectively protect the matrix material from further combustion.[54] The addition of PA-CS-Mn complex can also optimize the flame-retardant properties of the polymer. With its strong catalytic carbonization ability, which can effectively compensate for the looser carbon layer after the combustion of EG, a denser carbon layer formed. In short, phytic acid, chitosan, and metal complex can form a good cross-linking network, which can promote the carbonization process of EP, delay the quality and heat transfer in the combustion process, and greatly reduce the heat release rate of the material in the combustion.[55,56] In the gas phase, the PO· and PO_2· radicals produced by the decomposition of phytic acid can act as a physical barrier to capture the H· and OH· radicals generated during the combustion process and further destroy the combustion process. In addition, the nitrogen element in chitosan can also release a large amount of incombustible gases, such as N_2, NH_2, CO_2, which can efficiently dilute the combustible gas and oxygen concentration in the air, so as to achieve excellent flame retardant performance.[57,58] In summary, flame retardants in the gas phase and condensed phase together play a flame retardant effect, which greatly improves the thermal stability and flame retardant performance of the material, and better protects the matrix material.

4. Conclusion

In this study, phytic acid, chitosan and different metal ions were used to synthesize a PA-CS-M complexes as effective flame retardants in EP with a green and facile method. Among them, the CCT results shows that PA-CS-Mn can indeed improve the flame retardancy of the material, its pk-HRR value is reduced by 38%, SPR value is reduced by 33%, and it also has a significant inhibitory effect on toxic fumes such as CO. When combined with the traditional halogen-free and high-efficiency flame retardant of EG with the optimizing ratio of 1:5 (w/w), a high-quality expansible carbon layer is produced after combustion of EP composites, which can obviously reduce the pk-HRR

value by 69.8% and the SPR value by 66.6%. The degree of graphitization in the burning residues has also been significantly improved, which has indeed improved the thermal stability and smoke suppression properties of the material. In addition, the flexural modulus and flexural strength of the composites reached 5.04 GPa and 79.4 MPa, respectively. Compared with pure EP, it is significantly improved by 52.3% and 41.4%. The mechanical properties of the material have been greatly improved, and the scope of application of EP materials has been further expanded.

References

(1) Y. Yuan, Y. Q. Shi, B. Yu, J. Zhan, Y. Zhang, L. Song, C. Ma, and Y. Hu, *J. Hazard. Mater.*, **381**, 121233 (2020).
(2) Z. D. Zhang, J. Y. Qin, W. C. Zhang, Y. T. Pan, D. Y. Wang, and R. J. Yang, *Chem. Eng. J.*, **381**, 122777 (2020).
(3) J. Y. Dai, Y. Y. Peng, N. Teng, Y. Liu, C. C. Liu, X. B. Shen, S. Mahmud, J. Zhu, and X. Q. Liu, *ACS Sustain. Chem. Eng.*, **6**, 7589 (2018).
(4) A. Pomazi and A. Toldy, *Prog. Org. Coat.*, **151**, 106015 (2021).
(5) H. S. Ababsa, Z. Safidine, A. Mekki, Y. Grohens, A. Ouadah, and H. Chabane, *J. Polym. Res.*, **28**, 87 (2021).
(6) H. Yang, B. Yu, X. D. Xu, S. Bourbigot, H. Wang, and P. G. Song, *Green Chem.*, **22**, 2129 (2020).
(7) H. Wei, L. Li, Y. L. Ma, R. X. Liu, S. Y. Meng, L. T. Niu, Z. Zhang, and Z. W. Yang, *Fire Mater.*, **43**, 868 (2019).
(8) H. Wei, L. Li, X. X. Liang, R. X. Liu, Y. L. Ma, S. Y. Meng, Z. Zhang, Z. W. Yang, and Z. Q. Lei. *Mater. Res. Express.*, **6**, 085539 (2019).
(9) W. X. Li, H. J. Zhang, X. P. Hu, W. X. Yang, Z. Cheng, and C. Q. Xie. *J. Hazard. Mater.*, **398**, 123001 (2020).
(10) S. Yan, B. Luo, J. He, F. Lan, and Y. Wu. *J. Mater. Chem. B*, **9**, 1811 (2021).
(11) S. Alkandari, M. E. Bhatti, A. Aldughpassi, F. Al-Hassawi, M. Al-Foudari, and J. S. Sidhu. *Saudi J. Bio. Sci.*, **28**, 3602 (2021).
(12) M. Cegłowski, P. Balcerzak, R. Fránski, and G. Schroeder, *Eur. Mass Spectrom.*, **22**, 245 (2016).
(13) Z. H. Zhang, X. J. Li, Z. Y. Ma, H. Z. Ning, D. Zhang, and Y. H. Wang, *Dalton T.*, **49**, 2 (2020).
(14) L. E. Nita, A. P. Chiriac, A. Ghilan, A. G. Rusu, N. Tudorachi, and D. Timpu, *Int. J. Bio. Macromol.*, **181**, 561 (2021).
(15) A. P. M. Bloot, D. L. Kalschne, J. A. S. Amaral, I. J. Baraldi, and C. Canan, *Food Rev. Int.*, **6**, 1 (2021).
(16) Y. Y. Gao, C. Deng, Y. Y. Du, S. C. Huang, and Y. Z. Wang, *Polym. Degrad. Stabil.*, **161**, 298 (2021).
(17) C. K. Kundu, Z. W. Li, X. H. Li, Z. J. Zhang, and Y. Hu, *Int. J. Bio. Macromol.*, **156**, 362 (2020).
(18) Z. Q. Xiong, Y. Zhang, X. Y. Du, P. G. Song, and Z. P. Fang, *ACS Sustain. Chem. Eng.*, **7**, 8954 (2019).
(19) S. Ullah, F. Ahmad, A. G. Al-Sehemi, M. A. Assiri, M. R. Raza, and A. Irfan, *J. Appl. Polym. Sci.*, **138**, 50310 (2020).
(20) L. Maddalena, F. Carosio, J. Gomez, G. Saracco, and A. Fina, *Polym. Degrad. Stabil.*, **152**, 1, (2018).
(21) Y. Fang, W. Sun, J. Li, H. Liu, and X. Liu, *Int. J. Bio. Macromol.*, **175**, 140 (2021).
(22) X. W. Cheng, J. P. Guan, X. H. Yang, R. C. Tang, and F. Yao, *J. Clean. Prod.*, **223**, 342 (2019).
(23) S. Q. Li, R. C. Tang, and C. B. Yu, *Polym. Degrad. Stabil.*, **196**, 109826 (2022).
(24) G. Makhlouf, A. Abdelkhalik, and H. Ameen, *Prog. Org. Coat.*, **163**, 106627 (2022).
(25) S. Hu, L. Song, and Y. Hu, *Polym.-Plast. Technol.*, **52**, 393 (2013).
(26) M. Hassan, M. Nour, Y. Abdelmonem, G. Makhlouf, and A. Abdelkhalik, *Polym. Degrad. Stabil.*, **133**, 8 (2016).
(27) Y. Zhang, Z. Q. Xiong, H. D. Ge, L. K. Ni, T. Zhang, S. Q. Huo, P. G. Song, and Z. P. Fang, *ACS Sustain. Chem. Eng.*, **8**, 6402 (2020).
(28) R. Chen, Z. J. Luo, X. J. Yu, H. Tang, Y. Zhou, and H. Zhou, *Carbohyd. Polym.*, **245**, 116530 (2020).
(29) W. T. Li, S. K. Qi, Q. L. Liu, H. H. Gao, S. H. Liang, W. J. Feng, and M. J. Jiang, *J. Polym. Res.*, **27**, 1 (2020).
(30) W. Li, S. K. Qi, Q. L. Liu, H. H. Gao, S. H. Liang, W. J. Feng, and M. J. Jiang, *Int. J. Bio. Macromol.*, **140**, 303 (2019).
(31) X. D. Qian, C. L. Shi, and J. Y. Jing, *RSC Adv.*, **10**, 27408 (2020).
(32) J. Phanthuwongpakdee, T. Harimoto, S. Babel, S. Dwivedi, K. Takada, and T. Kaneko, *Polym. Degrad. Stabil.*, **188**, 109571 (2021).
(33) F. Zhang, W. Q. Liu, C. H. Liu, S. Wang, H. Y. Shi, L. Y. Liang, and K. Pi, *Colloid. Surfaces A.*, **617**, 126390 (2021).
(34) G. Y. Liu, H. L. Shi, C. K. Kundu, Z. W. Li, X. H. Li, and Z. J. Zhang, *J. Appl. Polym. Sci.*, **137**, 49601 (2020).
(35) W. H. Meng, Y. L. Dong, J. H. Li, L. Y. Cheng, H. J. Zhang, C. Z. Wang, Y. H. Jiao, J. Z. Xu, J. W. Hao, and H. Q. Qu, *Compos. Part B-Eng.*, **188,** 107854 (2020).
(36) K. M. Ossoss, M. E. R. Hassan, and A. S. Al-Hussaini, *J. Polym. Res.*, **26**, 199 (2019).
(37) A. S. Al-Hussaini, K. R. Eltabie, and M. E. R. Hassan, *Polym. Int.*, **67**, 1419 (2018).
(38) A. S. Al-Hussaini, *Polym. Bull.,* **76**, 323 (2019).
(39) A. S. Al-Hussaini, *High Perform. Polym.*, **26**, 166 (2014).
(40) A. S. Al-Hussaini, *Polym.-Plast. Technol.*, **55**, 1386 (2016).
(41) Y. Y. Wu, S. W. Zuo, Y. F. Zhao, H. Wang, D. Y. Li, S. Guo, Z. J. Zhao, J. Zhang, B. X. Hanab, and Z. M. Liu, *Green Chem.*, **22**, 1 (2020).
(42) Y. L. Sui, L. J. Qu, X. Y. Dai, P. H. Li, J. R. Zhang, S. Luo, and C. L. Zhang, *RSC Adv.*, **10**, 12492 (2020).
(43) A. S. Al-Hussaini, M. Klapper, T. Pakula, and K. Müllen, *Macromolecules*, **37**, 8269 (2004).
(44) A. S. Al-Hussaini, W. E. El-Bana, and N. A. El-Ghamaz, *Compos. Interfaces*, **27**, 385 (2020).
(45) J. Zhang, Z. Li, L. Zhang, Y. X. Yang, and D. Y. Wang, *ACS Sustain. Chem. Eng.*, **8**, 994 (2020).
(46) F. L. Hua, H. Wei, F. P. Ren, M. M. Wang, L. Li, B. L. Lv, H. Wang, Z.W. Yang, and Z. Q. Lei, *Fire Mater.*, **1**, 1099 (2021).
(47) L. Li, H. Wang, F. L. Hua, M. M. Wang, Y. S. Zhang, H. Xi, J. Yang, Z. W. Yang, Z. Q. Lei. *Mater. Res. Express*, **29**, 625 (2021).
(48) A. S. Al-Hussaini, K. R. Eltabie, and M. E. E. Rashad, *Polym. Int. J. Sci. Technol. Polym.*, **101**, 328-337 (2016).
(49) A. S. Al-Hussaini, K. M. Ossoss, and M. E. R. Hassan, *Polymer-Plastics Technology and Materials.*, **60**, 1331-1343 (2021).
(50) A. S. Al-Hussaini, A. M. Mohamedein, and M. E. R. Hassan, *J. Inorg. Organomet. Polym. Mater.*, **31**, 1491 (2021).
(51) A. S. Al-Hussaini, A. M. Elias, and M. A. A. El-Ghaffar, *J. Polym. Environ.*, **25**, 35 (2017).
(52) J. H. Zhang, X. Q. Mi, S. Y. Chen, Z. J. Xu, D. H. Zhang, M. H. Miao, and J. S. Wang, *Chemi. Eng. J.*, **381**, 122719 (2020).
(53) Y. L. Qin, M. C. Li, T. K. Huang, C. H. Shen, and S. J. Gao, *Polym. Degrad. Stabil.,* **195**, 109801 (2022).
(54) H. Wang, J. S. Cao, C. L. Cao, Y. Y. Guo, F. B. Luo, Q. R. Qian, B. Q. Huang, L. Xiao, and Q. H. Chen, *Polym. Adv. Technol.*, **30**, 493 (2019).
(55) Y. T. Wang, F. Wang, Q. X. Dong, W. J. Yuan, P. Liu, Y. F. Ding, S. M. Zhang, M. S. Yang, and G. Q. Zheng, *J. Appl. Polym. Sci.*, **135**, 46749 (2018).
(56) R. Goudarzi and G. H. Motlagh, *J. Macromol. Sci., Part B.*, **59**, 502 (2020).
(57) S. Kale, T. C. Nirmale, N. D. Khupse, B. Kale, M. V. Kulkarni, S. Pavitran, and S. W. Gosavi, *ACS Sustain. Chem. Eng.*, **9**, 1559 (2021).
(58) A. M. Chong, S. A. Salazar, and J. F. Stanzione III, *ACS Sustain. Chem. Eng.*, **9**, 5768 (2021).